

NATIONAL ADVISORY COMMITTEE FOR AERONAUTICS

TECHNICAL NOTE 4235

OBSERVATIONS OF TURBULENT-BURST GEOMETRY AND GROWTH IN SUPERSONIC FLOW

By Carlton S. James

Ames Aeronautical Laboratory
Moffett Field, Calif.

original paper copy from Ken Stetson, retired from AFFDL, Dayton, Ohio.
Scanned to 300 dpi, with images scanned to high-resolution gray scale by
Erick Swanson, May 2003. Images here captured are not available from
NASA STI or DTIC. S.P. Schneider, Purdue University, May 2003.



Washington

April 1958

SUMMARY

One step in the process of boundary-layer transition is the formation and spread of turbulent spots or bursts. A study of the shape, growth, and formation rate of turbulent bursts in supersonic boundary layers has been made using spark shadowgraphs of small gun-launched models in free flight through still air and through a countercurrent supersonic air stream. The shadowgraph data were obtained from a number of previous investigations which, collectively, represent a variety of model shapes, and a fairly wide range of Mach numbers, unit Reynolds numbers, surface roughnesses, and heat-transfer rates. The model shapes include cones, ogive-cylinders, and hollow cylinders aligned with the stream. The approximate ranges of the flow variables are as follows: free-stream Mach numbers from 2.7 to 10; unit Reynolds numbers from 1.6 million to 6.3 million per inch; surface roughness maximum peak-to-valley distance 10 microinches to 2100 microinches; and ratio of wall temperature to free-stream temperature either 1.0 (still air) or 1.8 (countercurrent air stream).

Three-dimensional burst geometry was determined for two typical turbulent bursts. From a comparison of burst plan forms and thickness profiles observed under different flow conditions, burst geometry was found to be insensitive to variation of Mach number, unit Reynolds number, and surface roughness. These variables, together with body shape, were found to have significant effects on the rate at which a burst is swept along the surface, its growth rate (relative to distance traveled), and the rate of burst formation.

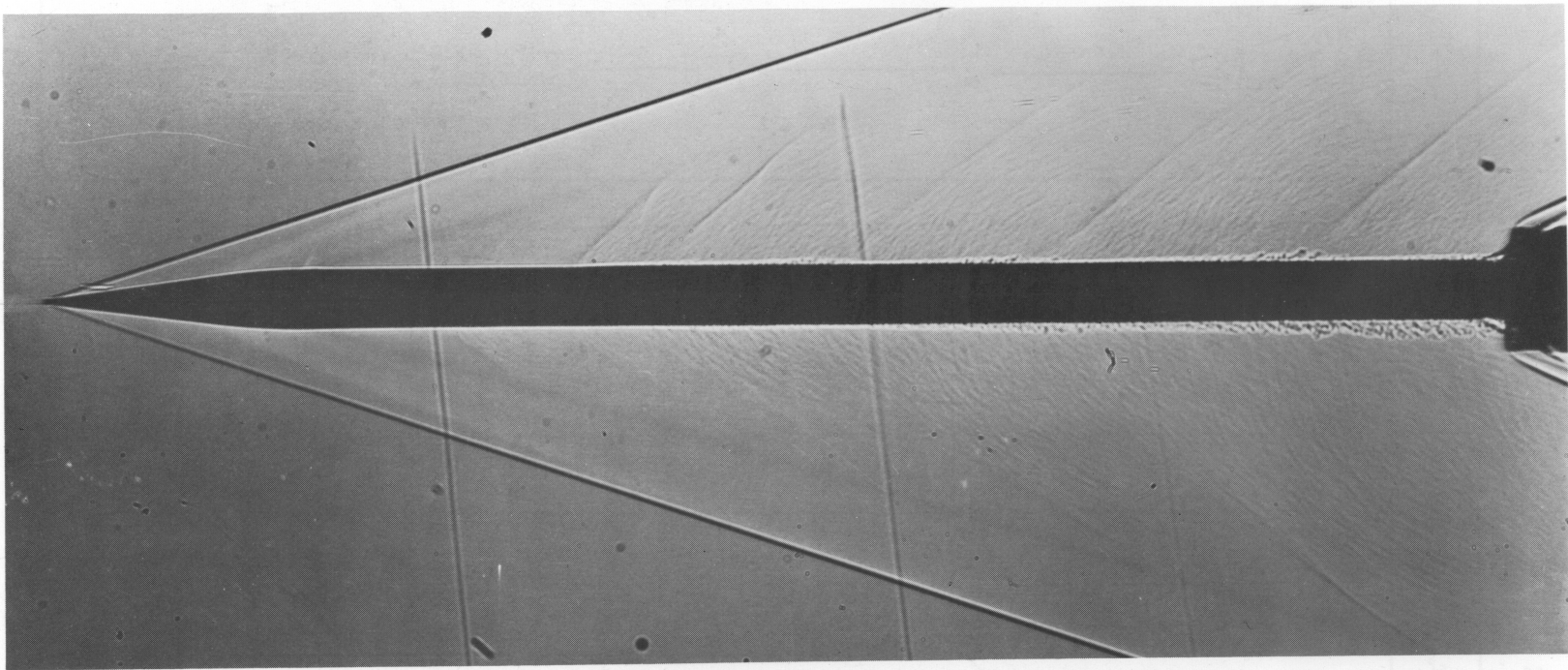
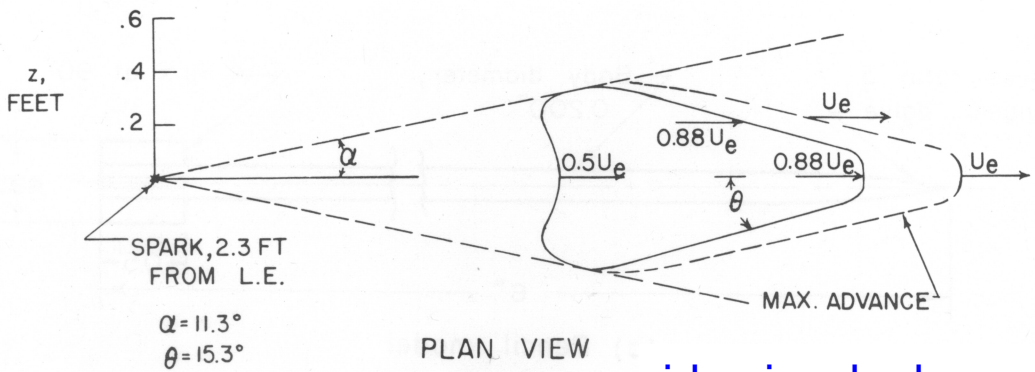
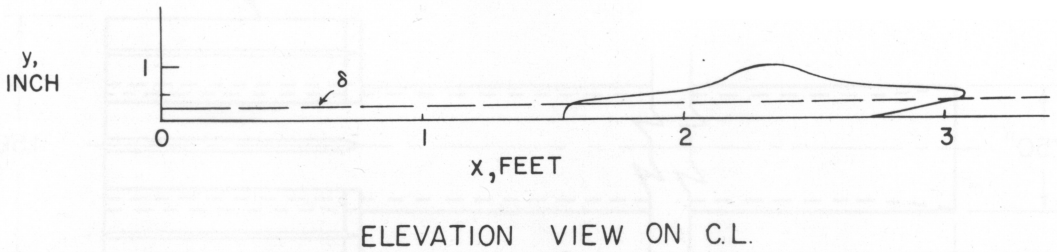


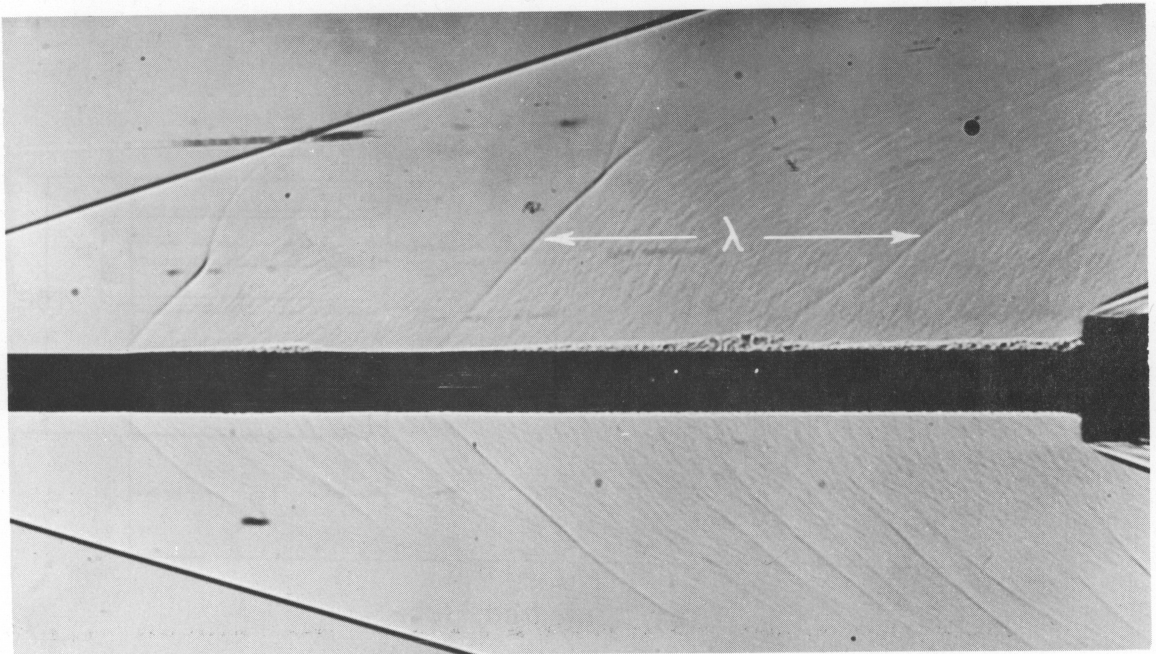
Figure 1.- Shadowgraph of conical-nosed cylinder model in free flight; $M_\infty = 3.5$; $U_e/\nu = 2.1 \times 10^6$ per inch; $H = 150 \mu\text{in.}$; wind tunnel "air-off"; conical light field.



side view looks similar

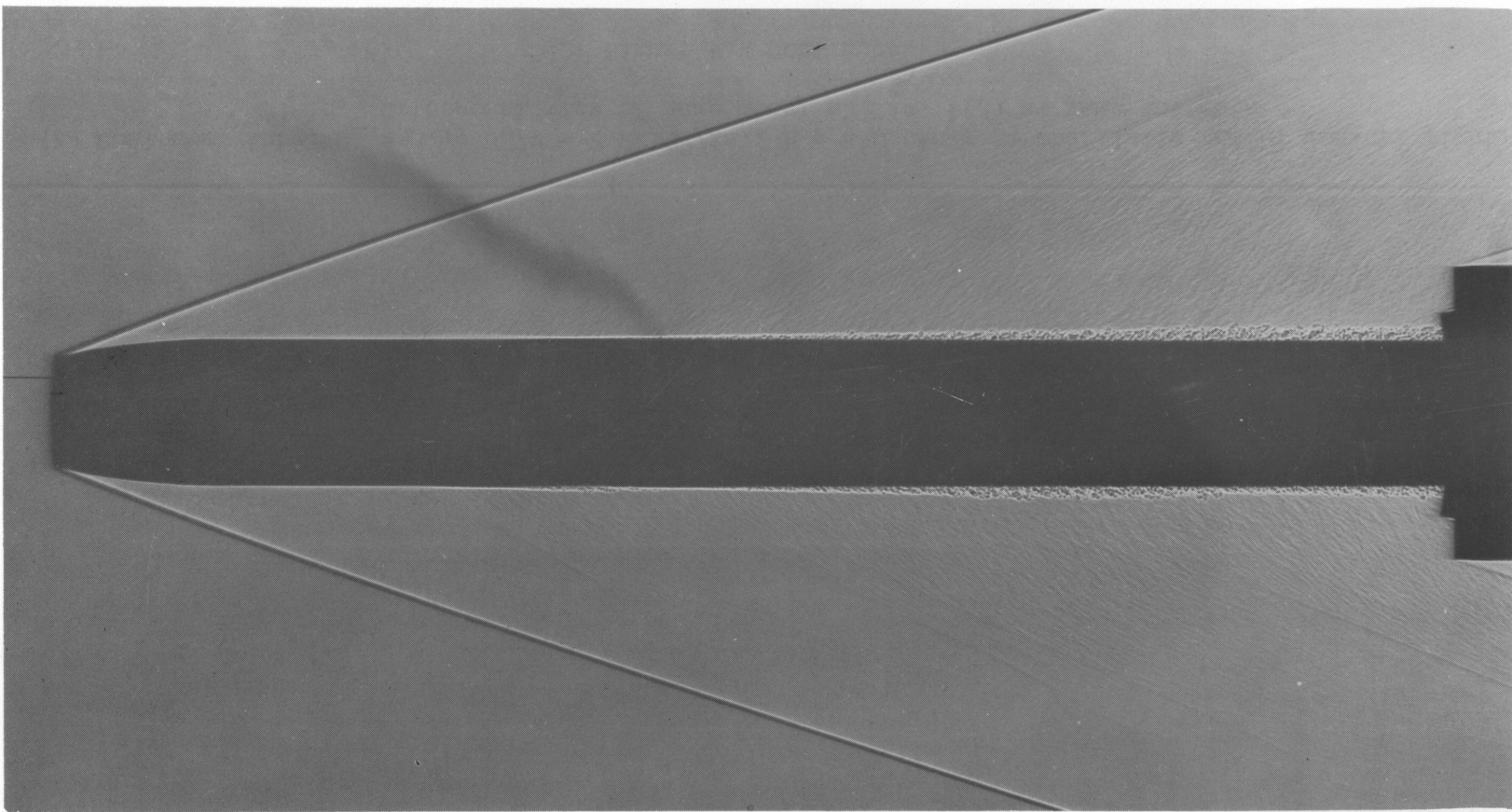


(a) Burst geometry and growth deduced from hot-wire measurements by Schubauer and Klebanoff (portion of fig. 6, ref. 5); $M_\infty \approx 0.03$; $U_e/\nu \approx 1.5 \times 10^4/\text{in.}$

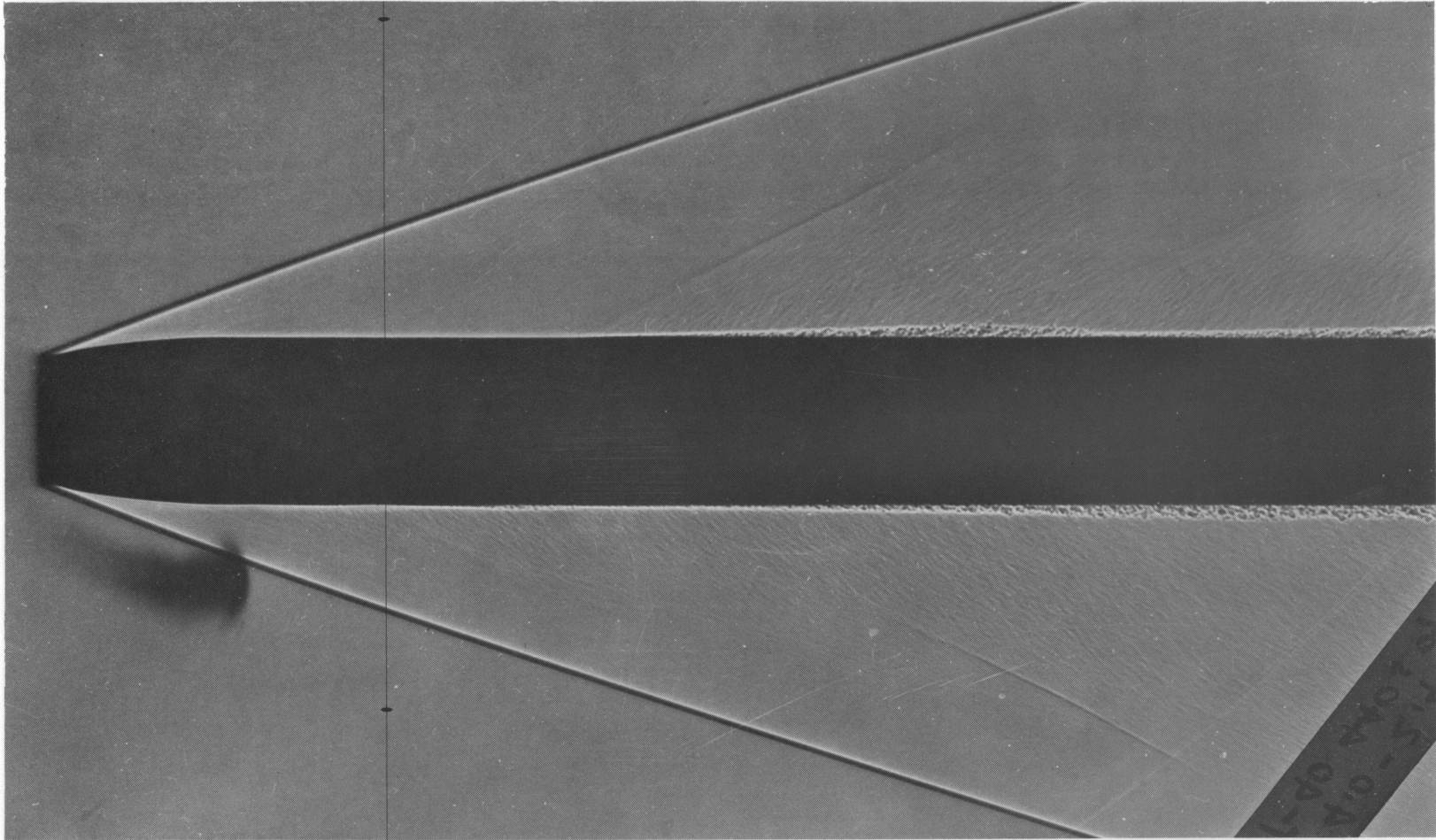


(b) Bursts on a slender ogive-cylinder (pencil model) in free flight; $M_\infty = 3.6$; $U_e/\nu = 3.6 \times 10^6/\text{in.}$; wind tunnel air-off; conical light field.

Figure 2.- Comparison of geometric characteristics of bursts observed under widely different flow conditions.



(j) Contoured tube; $M_\infty = 3.7$; $U_e/\nu = 2.2 \times 10^6/\text{in.}$; $H = 440 \mu\text{in.}$; aeroballistic range; conical light field. Orthogonal view of same model as fig. 4(k) at same instant.

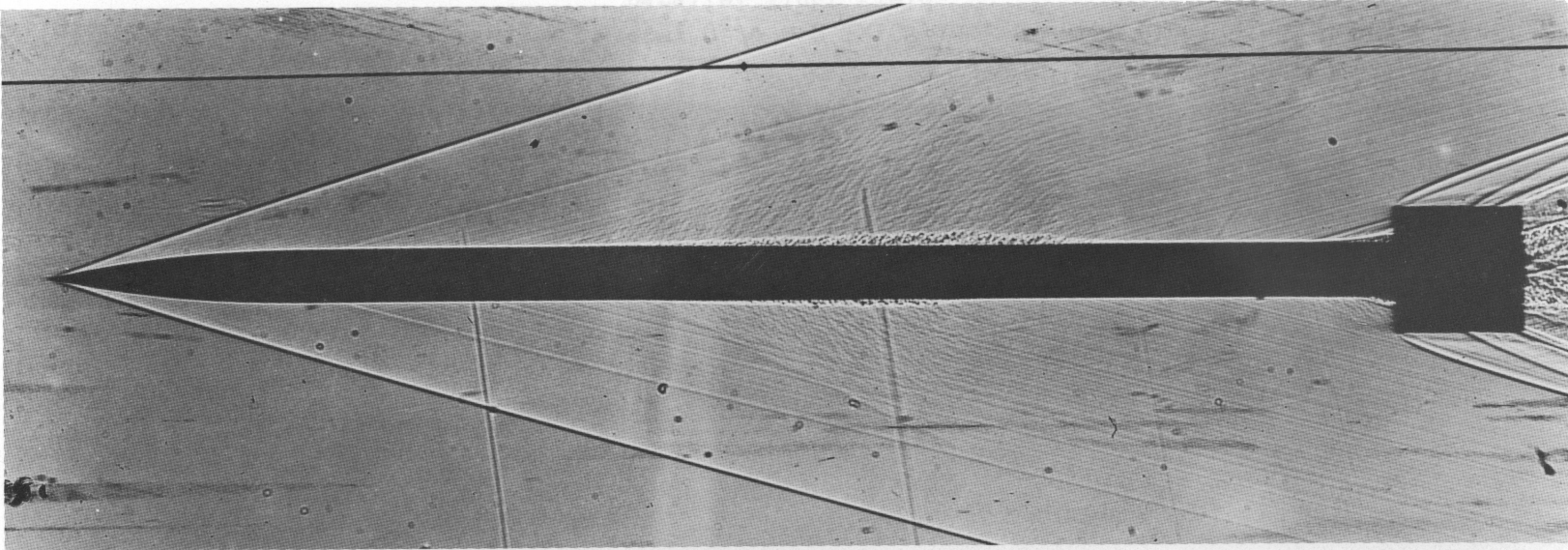


(k) Contoured tube; $M_\infty = 3.7$; $U_e/\nu = 2.2 \times 10^6/\text{in.}$; $H = 440 \mu\text{in.}$; aeroballistic range; conical light field. Orthogonal view of same model as fig. 4(j) at same instant.

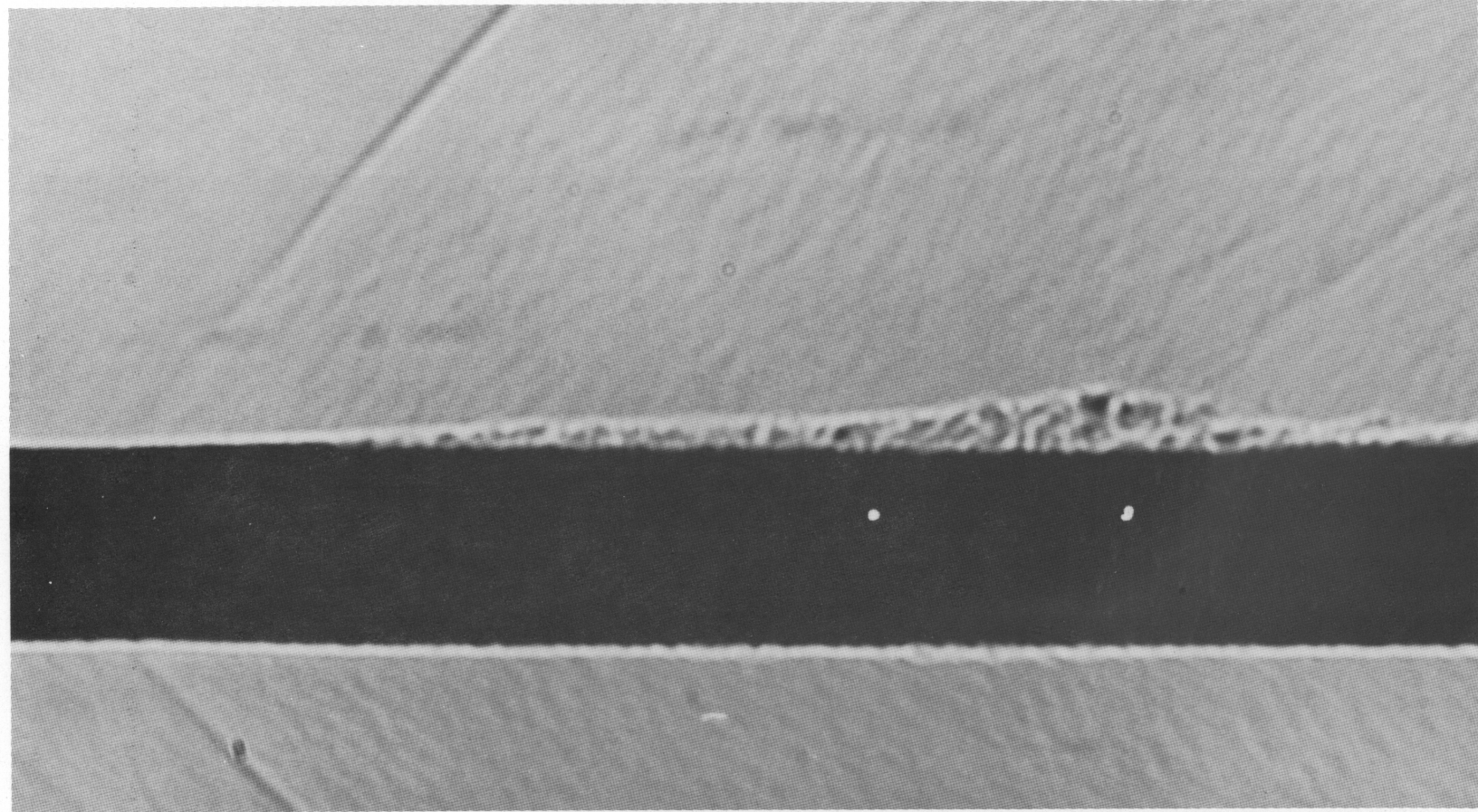


(l) Contoured tube; $M_\infty = 3.7$; $U_e/v = 2.2 \times 10^6/\text{in.}$; $H = 440 \mu\text{in.}$; aeroballistic range; conical light field. Same view of same model as fig. 4(j) but 0.0132 second later.

Figure 4.- Continued.

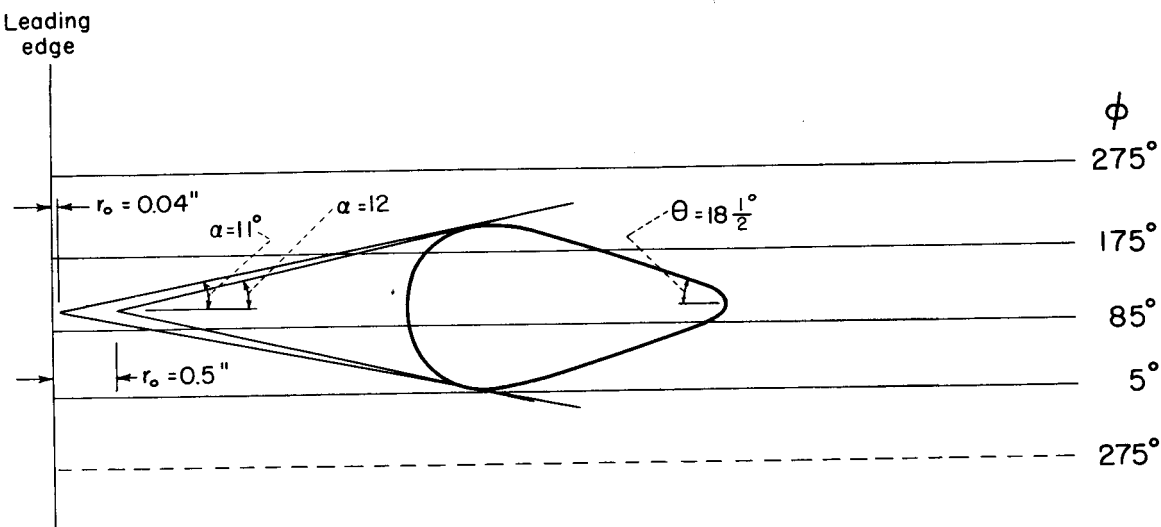


(p) Pencil model; $M_{\infty} = 3.9$; $U_e/\nu = 2.2 \times 10^6/\text{in.}$; $H = 700 \mu\text{in.}$; wind tunnel air-off; conical light field.

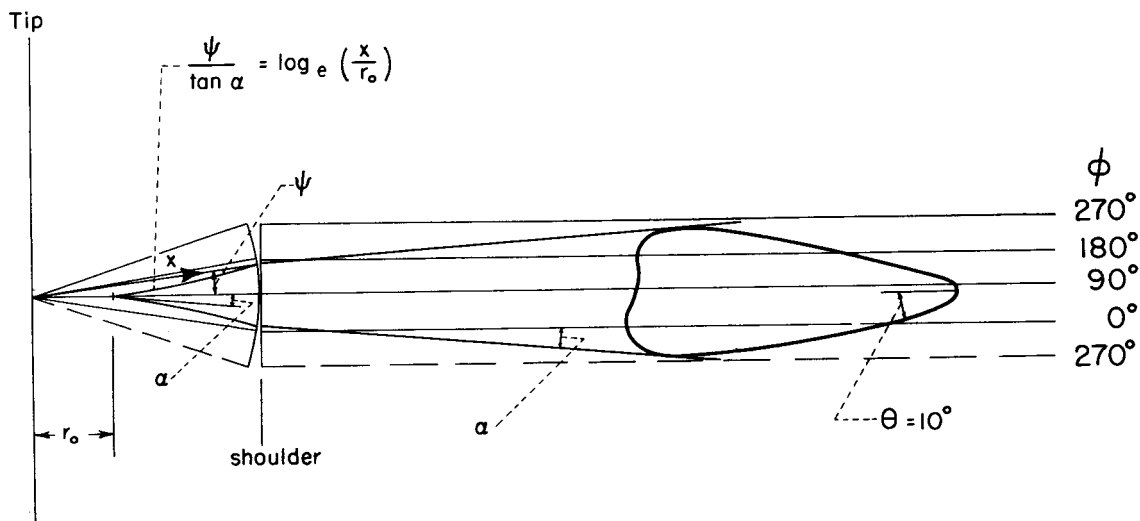


(a) Burst on pencil model; 5X.

Figure 6.- Enlarged shadowgraph profiles of bursts.

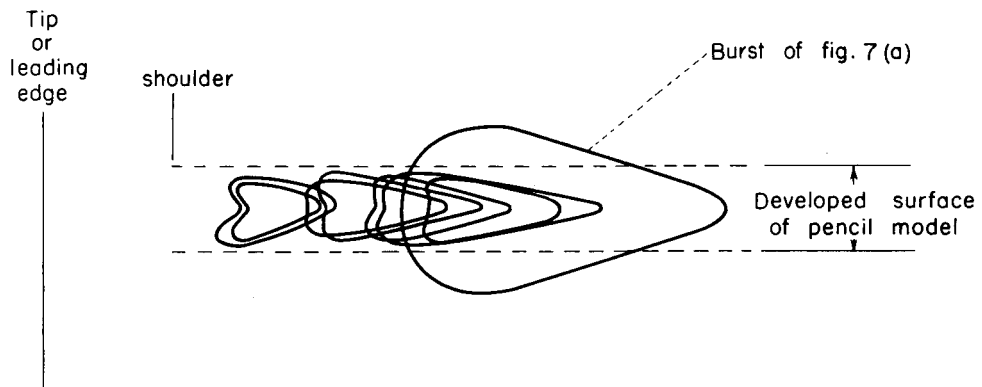


(a) Developed plan form of burst on the straight tube;
 $M_e = 3.9$; $U_e/\nu = 2.3 \times 10^6/\text{in.}$

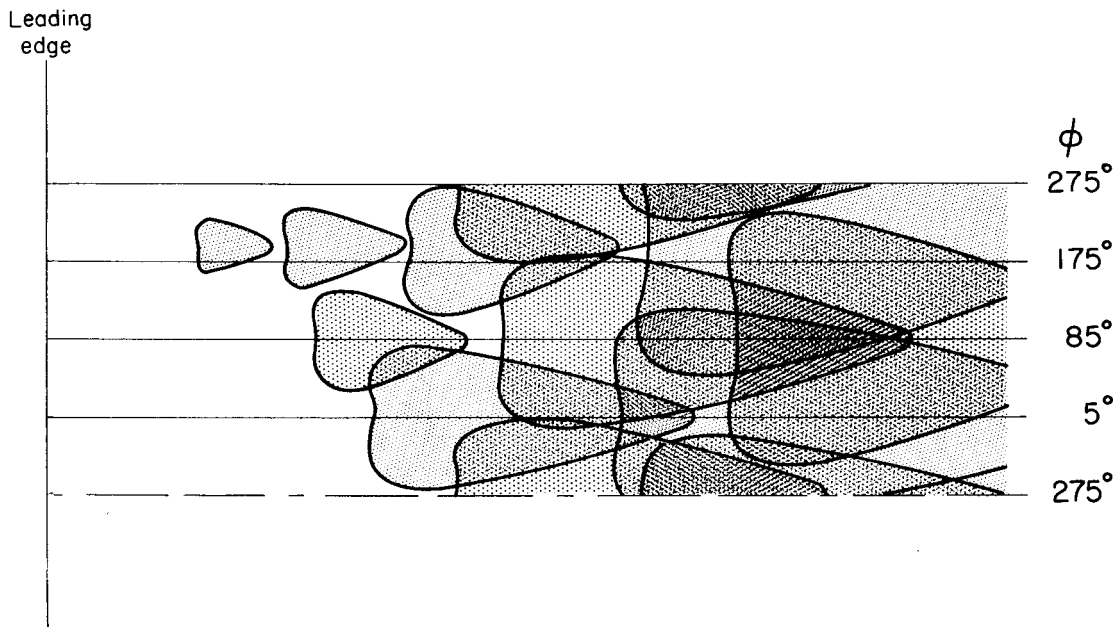


(b) Developed plan form of burst on the pencil model;
 $M_e = 3.5$; $U_e/\nu = 2.0 \times 10^6/\text{in.}$

Figure 7.-Burst plan forms determined from shadowgraphs.



(c) Composite of developed burst plan form.



(d) Distribution of bursts on developed surface of contoured tube.

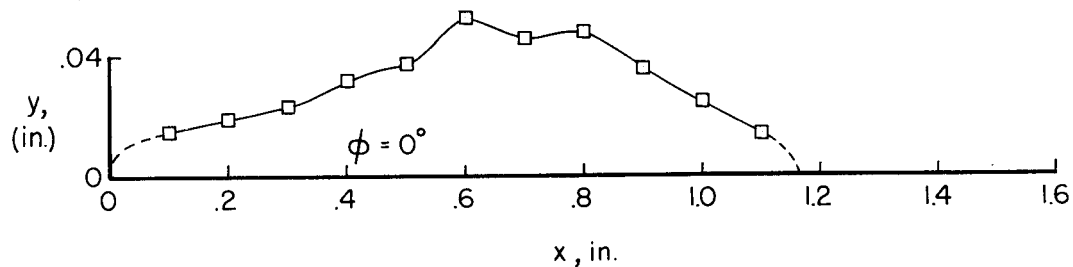
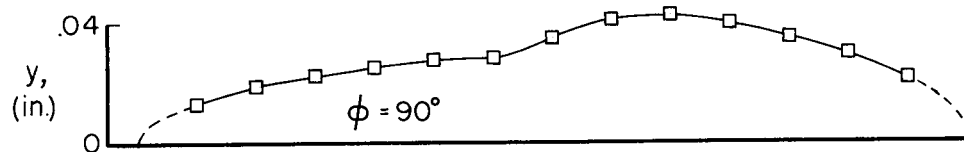
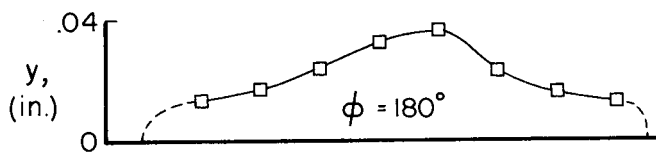
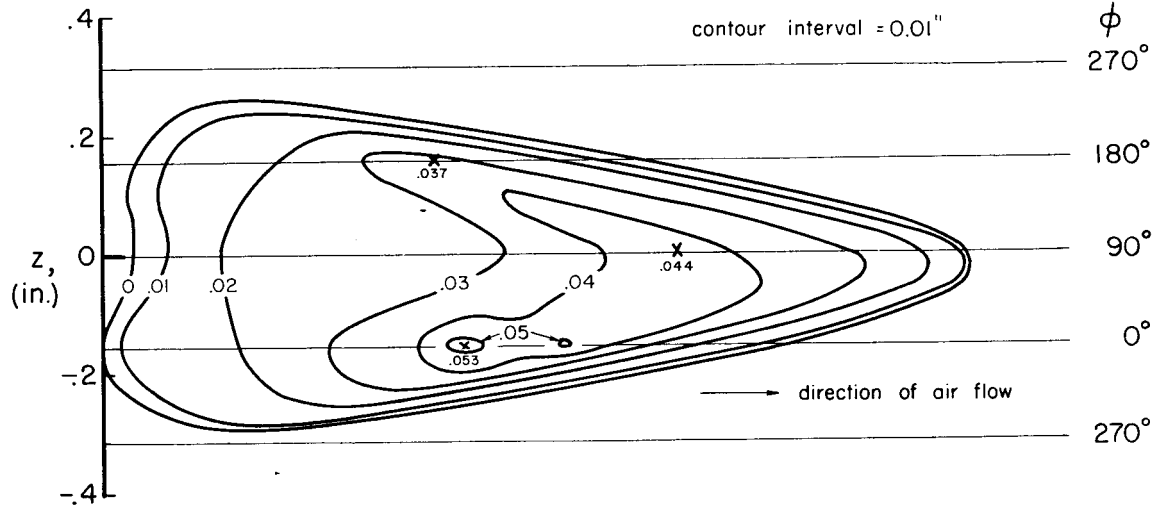


Figure 8.- Contour map and meridian profiles of a burst on the pencil model ; $Me = 3.5$; $u_e/\nu = 2.0 \times 10^6/\text{in.}$

Tip is
never
perfect,
flaws are
important!

(a) 19° included-angle cone; orthogonal views of the same tip.

(b) 19° included-angle cone.

(c) Pencil model.

Figure 20.- Photomicrographs of model tip profiles; 300X.